

A Comparison Of Voltage-Mode Soft-Switching Methods for PWM Converters

K. Mark Smith Jr. and Keyue M. Smedley
Dept. of Electrical and Computer Engineering
University of California, Irvine
Irvine, California 92697

Abstract - A comparison study was conducted to characterize the loss mechanisms, component stresses, and overall efficiencies of a group of voltage-mode soft-switching PWM methods including two newly developed methods. All soft-switching methods in the selected group allow zero voltage turn-on and turn-off of the main switch and utilize a single auxiliary switch with some resonant components. Advantages and disadvantages are identified for each method. Experimental verification for each soft-switching method are provided. It was found that not all the existing methods improved efficiency over most of the load range, but only those methods that softly switch the auxiliary switch, minimize redirection current, and recover the auxiliary circuit energy.

I. INTRODUCTION

High frequency operation of PWM converters allow reduction of the size and weight of their magnetic components. However, at high switching frequency, switching losses and EMI emissions become significant and must be reduced. Take the PWM boost converter as an example. The diode's passive switching characteristics cause large power spikes in the main switch during the turn-on and turn-off intervals by forcing the main switch to have simultaneous non-zero current and voltage [15]. Furthermore, because of the reverse recovery of the diode during the main switch turn-on interval, there is a shoot through of the output capacitor to ground, causing a substantial current spike through the diode and main switch. Another loss element associated with the switch is the built up charge in the device which dissipates in the switch during turn-on. For MOSFETs, this drain to source charge is substantial and contributes further to the switching losses. These switch turn-on and turn-off losses increase linearly with switching frequency and must be reduced in order to take advantage of the high switching frequency PWM converters.

In recent years, many voltage-mode soft-switching techniques have been proposed [2,3,4,5,6,7,8,9,10,11,12] and show promising solutions to the switching and the shoot through problems of high frequency PWM converters. These methods enable the main switch to be turned on and off at zero voltage. They are most notably helpful with MOSFET devices because they reduce the substantial losses associated

with turn-on of the MOSFET switch. Zero voltage soft-switching techniques have also been used with IGBTs with improved performance [4,13,14].

In this paper, a group of voltage-mode soft-switching converters utilizing an auxiliary switch with an inductor were selected to do an efficiency comparison. These methods intend to improve the PWM efficiency by allowing the main switch to be turned on and off with zero voltage and controlling the diode's turn-off transient. Even though the losses in the main switch are dramatically reduced, the auxiliary circuits will add some additional losses to the converter. Therefore, to improve the overall efficiency of the converter, the losses in the auxiliary circuit must be smaller than the energy savings from the soft-switching of the main switch. Identification of these losses within the auxiliary circuit are crucial to engineering applications. It is the aim of this paper to compare these soft-switching techniques including the two improvement circuits developed at UCI. The advantages and disadvantages of each method are identified and verified through experimental tests. The overall efficiency of the methods are examined with the consideration of the conduction and switching losses present in the auxiliary and main circuit. Section II describes the general theory behind the compared techniques. Section III describes the five different methods. Section IV discusses the experimental setup and procedure. Section V shows the experimental comparison and section VI gives a summary.

II. GENERAL APPROACH OF VOLTAGE-MODE SOFT-SWITCHING WITH AN AUXILIARY SWITCH

Figure 1 shows a basic boost converter. The commutation between the outlined two switches is influenced by the direction of the inductor current. To facilitate a general discussion of voltage-mode soft-switching methods, Fig. 2 shows two switches with a current source that can represent the switches of the basic switch converter topologies (boost, buck, buck-boost, Half-bridge, etc.). The current source, I_s , models either the filter or energy transfer inductor associated with the converter type. Without loss of generality, I_s in Fig. 2 is shown in the direction towards node a , similar to a boost converter. The switches are either both active or one active, one passive. For the boost converter, S_2 is usually a diode and S_1 will be an active switch. Two snubber capacitors, C_1 and C_2 , are placed across the switches

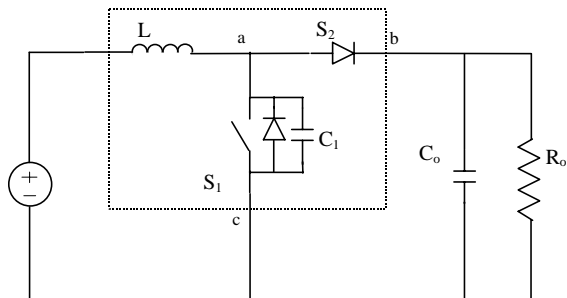


Fig. 1. Basic boost converter

to help with zero voltage switching. Zero-voltage soft-switching can always be performed for one switching direction by utilizing the current source to charge and discharge the snubber capacitors placed across the switches. Assume that S_1 is conducting and S_2 is off. If S_1 is turned off, the current source, I_s , will charge C_1 and discharge C_2 . This allows S_1 to be turned off softly. When the voltage at node a , V_a , reaches the voltage at node b , V_b , the snubber capacitor, C_2 , across S_2 reaches zero voltage and the anti-parallel diode will be turned on. If S_2 is active, it can be turned on at this time with zero voltage. Because of the direction of I_s , natural zero-voltage switching is not possible during the S_2 to S_1 commutation. In this case, zero-voltage switching is performed with the help of additional circuit elements.

To achieve zero voltage switching during the S_2 to S_1 commutation, a redirection current i_r must first be switched into node a softly (Fig. 3.). The growth of the redirection current causes the current through S_2 to reduce so that $i_r + i_{S2} = I_s$. Furthermore this redirection current must grow larger than I_s during the transient so that i_{S2} will change directions allowing S_2 to be turned off with zero voltage. If S_2 is just a diode, the reverse recovery current will be controlled by the redirection current i_r . After S_2 is turned off, the redirection current charges C_2 and discharges C_1 , which cause the voltage at node a to drop. When the voltage at node a reaches the voltage at node c , V_c , the anti-parallel diode of the main switch S_1 will conduct allowing S_1 to be turned on with zero voltage.

Figure 4 shows how this additional current is realized for the voltage-mode soft-switching methods presented in this

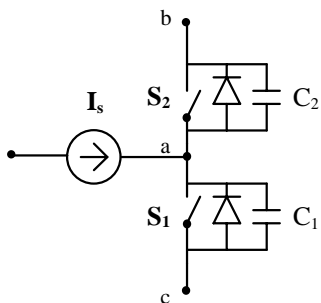


Fig. 2. A two switch converter

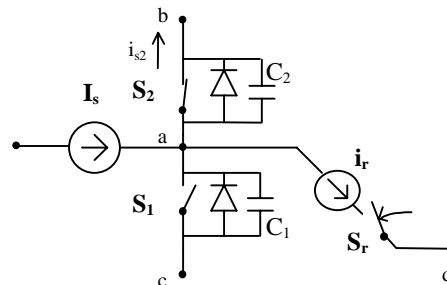


Fig. 3. converter with redirection current

paper. The redirection current i_r , is actualized by a small inductor being switched into the circuit from any another node in the circuit, say node d , with a different voltage level. For Fig. 4, the voltage at node d , V_d , must be lower than the voltage at node a , V_a , to realize the correct current direction for soft-switching. When the auxiliary switch, S_r , is closed, and $V_d < V_a$, then the current will increase linearly according to the following equation:

$$i_{Lr}(t) = \frac{(V_a - V_d)t}{L_r} \quad (1)$$

When i_r reaches I_s , the current in S_2 reaches zero and will change direction if it is not a diode. After this time S_2 can be turned off. The equivalent circuit now contains at the very least resonant elements C_1 , C_2 and L_r . Two of the selected circuits (Methods D and E) include an additional resonant capacitor to help transfer the inductor energy and will be discussed later. In any case, particular circuit conditions must be satisfied to allow the C_1 voltage to resonate to zero volts. For an auxiliary circuit with just an inductor and a switch, the equivalent circuit model when S_r is closed and S_2 is opened is shown in Fig. 5. The initial voltage across C_1 and C_2 is $V_b - V_c$ and zero respectively, and the initial inductor current is I_r . Solving this circuit gives the following equation for $V_{C1}(t)$ where $C_e = C_1 + C_2$ and $\Delta I = I_r - I_s$:

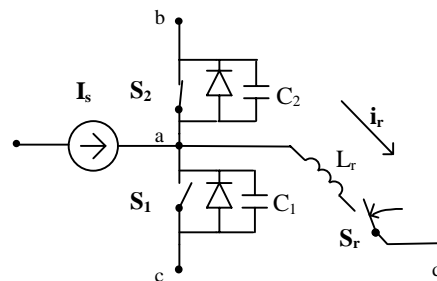


Fig. 4. converter with auxiliary switch.

$$V_{C1}(t) = V_d - V_c + (V_b - V_d) \cos\left(\frac{t}{\sqrt{C_e L_r}}\right) + \Delta I \sqrt{\frac{L_r}{C_e}} \sin\left(\frac{t}{\sqrt{C_e L_r}}\right) \quad (2)$$

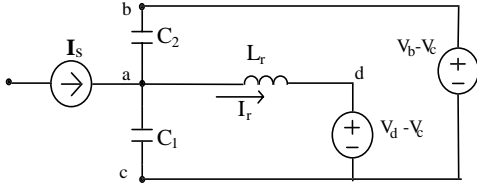


Fig. 5. Equivalent circuit

In the case when both switches are active, $\Delta I > 0$ is dependent on the time between the turn off of S_2 and the turn on of S_1 . For all the compared methods switch S_2 is a diode; therefore, this passive switch will turn off when the inductor current equal I_s , i.e. $\Delta I = 0$. When $\Delta I = 0$, the zero voltage condition of C_1 is found from (2) as follows:

$$V_d < \frac{V_b + V_c}{2} \quad (3)$$

Once the zero voltage switching is achieved, L_r contains energy from C_1 and the input current I_s . This energy may be transferred back into the main power processing path (i.e. input or output) or dissipated internally within the auxiliary circuit. Each one of the auxiliary circuits in the selected group uses different mechanisms for recovering or dissipating this inductor energy.

To achieve higher overall circuit efficiency, the auxiliary circuit must have less losses than the amount of energy savings resulting from the soft-switching of the main switches. The losses within the auxiliary circuit include the conduction, turn-on and turn-off losses of the auxiliary switch. Because the selected methods use an inductor to generate the current redirection, the auxiliary switches are turned on with zero current. However, the turn-on voltage will not be zero according to (3), causing the switch to dissipate its own internally stored capacitive energy. Since all circuits in the selected group use a MOSFET switch, the internal C_{ds} capacitance is not negligible and effects the circuit efficiency. Additionally, in high voltage applications such as a power factor correcting boost input stage where the output voltage is greater than 100 volts, the conduction loss due to the on resistance of the auxiliary switch is also substantial. For the MOSFET auxiliary switch used in the experimental circuits (IRF840) the on resistance, r_{dson} , is about 1Ω . The turn-off of the auxiliary switch can also be lossy depending on the method used. These losses within the auxiliary circuit are dependent on the circuit current I_s and the voltage level V_b . When performing the experiments,

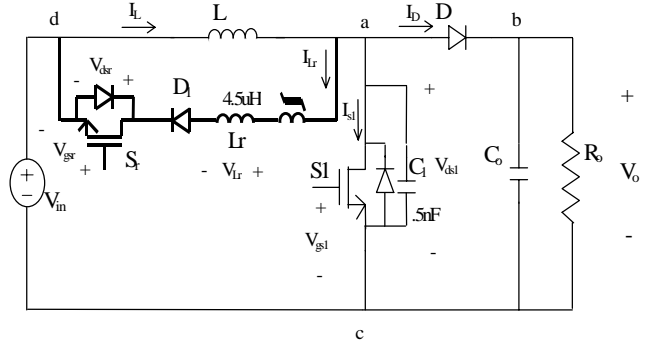


Fig. 6. Method A

these circuit parameters are matched between different zero voltage soft-switching methods, giving a fair comparison of each technique's losses. The auxiliary circuits compared allow zero voltage switching of the main switch, but each one has their own turn-on, turn-off, and conduction losses that effect the overall converter efficiency with varying amounts.

III. THE COMPARED METHODS

The operation, characteristics and loss mechanisms of 5 different voltage-mode soft-switching methods are discussed in this section. Losses due to the magnetic core and the diode are assumed small compared to the auxiliary switch losses. Therefore, when comparing the loss mechanisms, these effects are neglected, but do contribute partially to the losses in the circuit.

Method A

Figure 6 shows the schematic of this soft switching method. The location of the voltage nodes a, b, c, d from Fig. 4 are given as a reference to the discussions in the previous section. Although this soft switching method was independently created by the authors, a similar technique first appeared in [6] where analysis for the buck converter was given. This technique uses the least components off all the methods tested. Furthermore, it transfers C_1 's stored capacitor energy back to the input and has very small internal losses allowing for substantial efficiency improvement over the hard switched converter. The operational waveforms are given in Fig. 7. Notice that before time t_0 the main switch, S_1 , is off and the diode D is conducting the input current I_L . In order for the main switch to be turned on with zero voltage, the voltage across the switch and the capacitor C_1 must be forced to zero. To do this, at time t_0 , the auxiliary switch, S_r , is turned on, allowing the current in the resonant inductor, L_r , to rise linearly according to (1). Once the current in L_r reaches the input current level at t_1 , the diode D has a controlled reverse recovery and the equivalent circuit is identical to Fig. 5 with C_2 equal to zero Farads. As long as $V_o/V_{in} > 2$ (from (3)) then the voltage across the main switch and C_1 , V_{ds1} , will reach zero at t_2 and the main switch's anti-parallel diode will conduct. Once the anti-parallel diode conducts, the main switch can then be turned on with zero

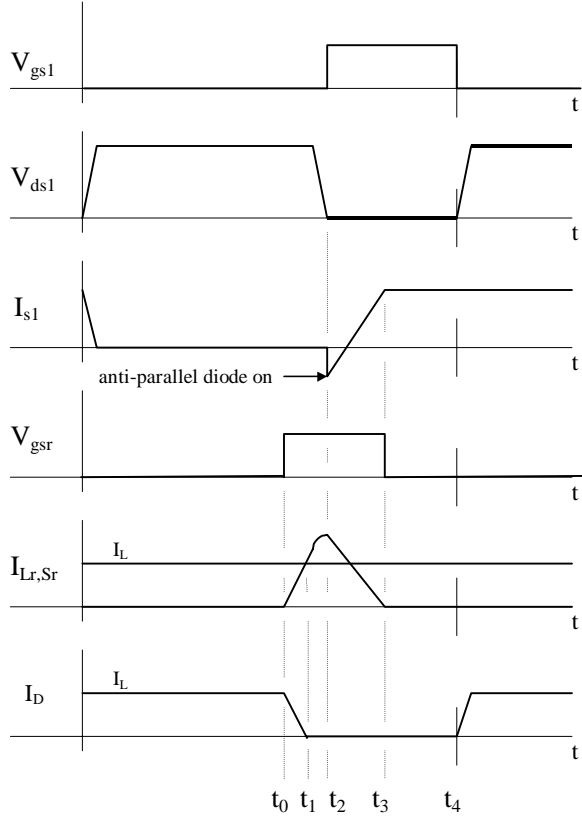


Fig. 7. Method A theoretical waveforms

voltage and is done so with the V_{gs1} gate drive signal. At this point the energy from the capacitor C_1 and additional energy from the input have been transferred into the auxiliary circuit and stored in the resonant inductor, L_r . However, during the resonant cycle between t_1 and t_2 the voltage across L_r reverses polarity from $(V_o - V_{in})$ to $-V_{in}$, automatically forcing the inductor current to return to zero amps at time t_3 . Therefore, the energy stored in L_r is transferred back to the input. Additionally, once the current in L_r reaches zero amps, the auxiliary switch is turned off softly with zero current by the diode D_1 . The gate drive to S_r can then be turned off (see V_{gsr}). Finally, at time t_4 the main switch is turned off softly with zero voltage by the auxiliary capacitor C_1 . The auxiliary switch turn-on and conduction losses are the two substantial losses present in this method. The auxiliary switch turn-on loss is defined by the following equation:

$$W_{on-loss} = \frac{1}{2} C_{ds} (V_o - V_{in})^2, \quad (4)$$

where C_{ds} is the parasitic capacitor of the auxiliary switch S_r . It is the lowest among all the methods compared. Since the turn-off is soft, the only other major loss element within the auxiliary circuit is the conduction loss due the switch. The experimental circuit also contained a saturable reactor to soften the diode D_1 's turn-off at t_3 .

Method B

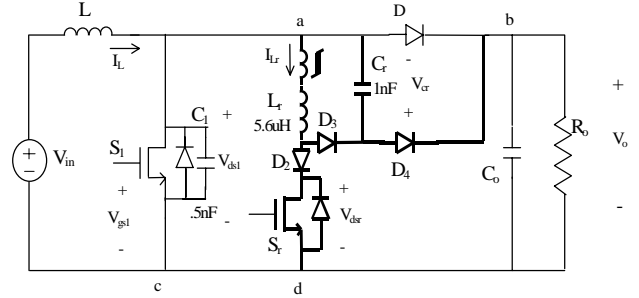


Fig. 8. Method B

The soft-switching boost converter shown in Fig. 8 and presented in [2] was the first technique to allow soft-switching and still keep the PWM voltage and current waveforms practically unchanged. Although [2] describes the technique for the boost converter, it can be applied to any of the popular topologies [3]. The operation of the auxiliary circuit is detailed in [2]. After S_r is turned on, the current in the inductor L_r will ramp up linearly until it reaches the input current level as described by (1) with $V_d = 0$. At this time the diode turns off under controlled di/dt . The equivalent circuit is the same as Fig. 5 except that $V_d = V_c = 0$. Also, constraint (3) is always satisfied ensuring that C_1 's voltage will reach zero and allow the anti-parallel diode to conduct. At this time S_1 is turned on softly. S_r is then turned off softly due to the snubber capacitor (C_r). The energy in L_r is then transferred into the snubber capacitor. If voltage across C_r reaches the output voltage, then D_4 will conduct. In any case, when the main switch is turned off, the snubber capacitor, C_r , is reset to zero volts through D_4 . The turn-on losses of the auxiliary switch are larger than with method A:

$$W_{on-loss} = \frac{1}{2} C_{ds} (V_o)^2 \quad (5)$$

However, the conduction losses through the auxiliary switch, S_r are less than that of method A because the switch is turned off as soon as C_1 reaches zero volts and does not conduct the complete auxiliary circuit cycle. These differences are significant and will be evident when looking at the experimental results. To soften the reverse recovery of D_3 when the current returns to zero amps, a saturable inductor was inserted in series with the inductor, L_r , as done in [4]. This replaces the dissipative snubber added to the circuit in [2].

Method C

Figure 9 shows a soft-switching converter presented in [4]. Operation is the same as method B, but uses less components by removing the capacitor snubber C_r . The saturable inductor in series with L_r helps with the reverse recovery of D_2 and D_3 . The energy lost at turn-on of S_r is identical to method B. Also, The conduction losses in the auxiliary switch are the same. However, because the C_r capacitor was removed, the auxiliary switch is turned off

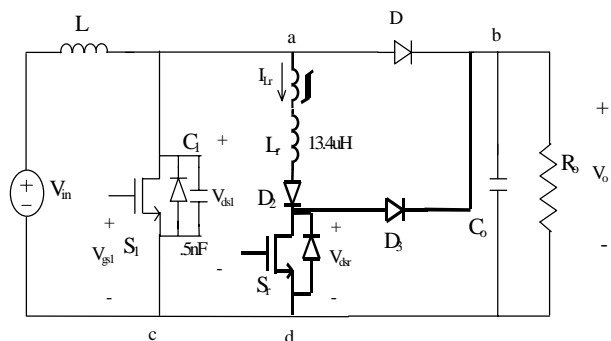


Fig. 9. Method C

dissipatively. This significantly reduces the efficiency compared to method B as shown in the experimental results.

Method D

Figure 10 shows the soft switching converter presented in [5]. Once again the location of the voltage nodes a, b, c, d from Fig. 4 are given. Two extra diodes were added to the auxiliary switch, S_r , to bypass its slow anti-parallel diode. The series diode blocks the anti-parallel diode from conducting and the parallel diode, D_1 , is essentially the new faster anti-parallel diode. It will be shown below that this is necessary to protect the auxiliary switch from possible voltage breakdown. One important difference this circuit has compared to the previous methods is the extra capacitor, C_r , in series with the resonant inductor, L_r . The capacitor allows for an LC resonance between L_r and C_r to return the inductor current to zero amps. Unlike Method B and C, this resonance does not require the auxiliary switch to turn-off in order to change the inductor current direction. However, in this method, the energy extracted from the main energy path to form the redirection current is not transferred to the input or output. Instead it is partially stored in C_r and the rest is dissipated internally. If the circuit was lossless, the C_r capacitor voltage would increase each switching cycle by an incremental amount until S_r breaks down. In practice, the incoming energy is balanced by the circuit conduction loss and auxiliary switch turn-on loss. A brief description of the

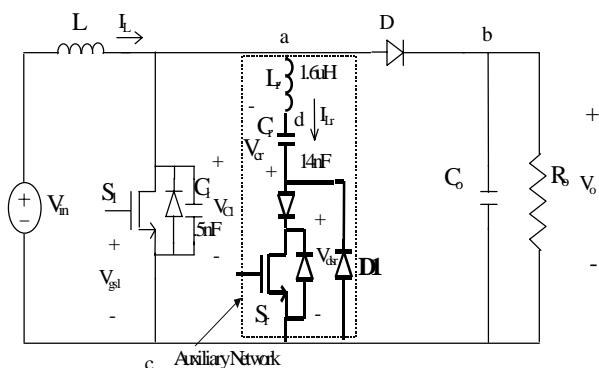


Fig. 10. Method D

circuit is given here with the theoretical waveforms shown in Fig. 11. Assume for now that the stored energy in C_r has a polarity shown in Fig. 10 and that the main switch is off. At t_0 , S_r is turned-on to form a redirection current through the inductor L_r . Even though this is an LC resonant circuit, because C_r is large enough, the inductor current, I_{L_r} , will change much faster than the capacitor voltage. In this case, equation (1) can still be used as an approximation of the inductor current increase with $V_a - V_d = V_o + V_{cr}$. As the inductor current increases, the C_r capacitor voltage will decrease from its initial value. Once I_{L_r} reaches the input current level, I_L , at t_1 the diode D has a controlled reverse recovery. This creates an LCC resonant circuit between C_1 , L_r , and C_r with the input current as the driving force. The voltage across L_r is still positive and so the current will continue to increase causing the capacitor voltages across C_1 and C_r to decrease. The zero voltage switching constraint given by (3) does not apply here due to the addition of C_r , however with the appropriate circuit parameters, zero voltage switching is realizable over most of the load range [5]. Once the voltage across C_1 decreases to zero at t_2 the main switch's anti-parallel diode will conduct allowing it to be turned on with zero voltage. With the anti-parallel diode conducting, L_r and C_r now make up an LC resonant circuit where the inductor current is substantially greater than the input current and C_r has decreased from its original voltage. The resonance between L_r and C_r forces the inductor current to return to zero at t_3 and changes conduction direction through diode D_1 . When the inductor current passes zero the voltage across the capacitor, C_r , is at its negative maximum with respect to the polarity shown in the schematic. With the inductor current negative and the diode D_1 conducting, the auxiliary switch can be turned off ideally with zero voltage and zero current. The inductor current continues negative performing a half resonant cycle and returns to zero amps at t_4 where it stops because of the diode D_1 and S_r being off. During this half resonant cycle the C_r capacitor voltage has reversed directions and now contains the same polarity as it started with. Additionally, during this half cycle the main switch experiences a controlled current hump waveform. From [5] this peak current can be more than three times the input current and gives rise to additional conduction losses both in the auxiliary circuit and the main switch. Furthermore, when this current returns to zero, the reverse recovery time of the anti-parallel diode will allow a small forward inductor current. When the diode does recover, there will be a large voltage spike across the auxiliary switch, as evident in the experimental waveforms (Fig. 16). The added fast recovery anti-parallel diode, D_1 help to decrease this voltage spike. Since the energy brought into the auxiliary circuit is not recovered, it is partially dissipated by the S_r switch turn on loss, making this particular loss element the largest of any of the methods:

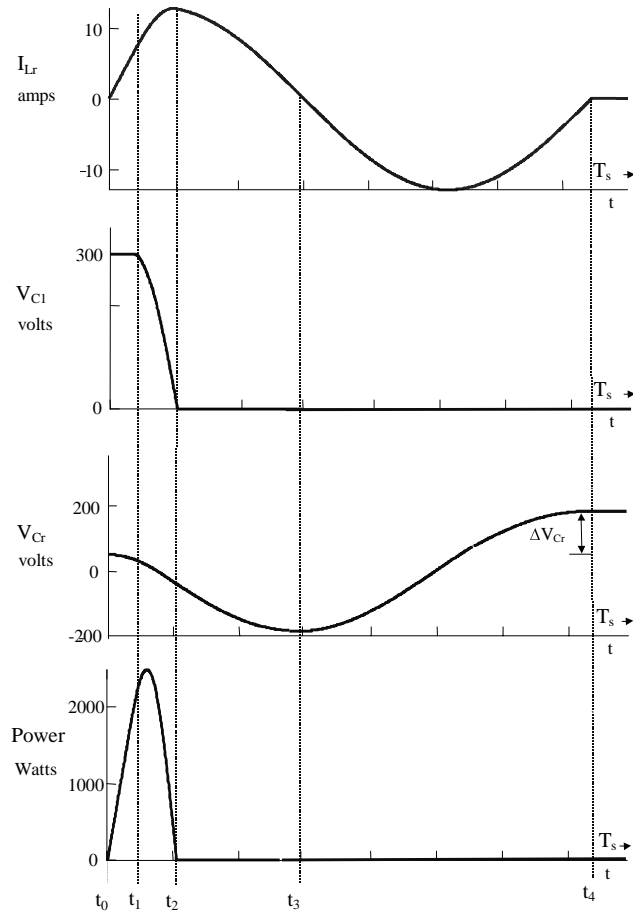


Fig. 11. Theoretical waveforms and power delivered to auxiliary circuit.

$$W_{on-loss} = \frac{1}{2} C_{ds} (V_o + V_{cr})^2 \quad (6)$$

To further illustrate the dissipative nature of this technique, Fig. 11 shows a graph of the theoretical power delivered to the auxiliary network outlined in Fig. 10 by the dotted box. Power is delivered to the network each cycle and never recovered. This cycle by cycle accumulated energy, ΔW , is seen by the increase in the C_r capacitor voltage, ΔV_{cr} , at the end of the cycle:

$$\Delta W = \frac{1}{2} C_r \Delta V_{cr} [V_{cr}(t_0) + \Delta V_{cr}] \quad (7)$$

In the experimental circuit, this incoming energy is balance by internal losses each cycle to reach a steady state solution.

Method E

A modification by the authors to the circuit in Fig. 10 yielded a new circuit shown in Fig. 12 with improved efficiency and component stress. By convention, node d from Fig. 4 is shown after the inductor although the capacitor C_r

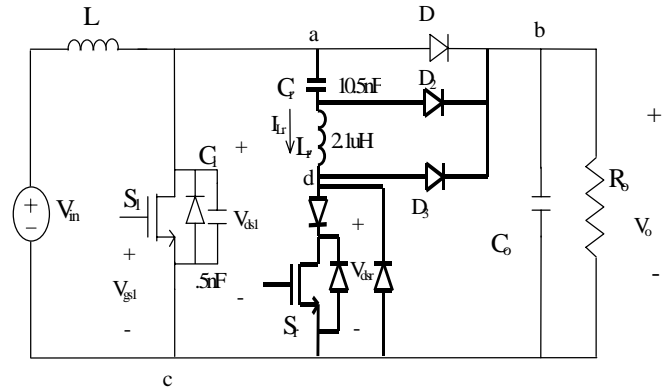


Fig. 12. Method E

has changed positions. This circuit adds two extra diodes, D_2 and D_3 . Diode D_2 allows the C_r capacitor voltage to be returned to zero volts every cycle there by transferring the added energy, (7), to the output each cycle and does not allow it to accumulate. Additionally, diode D_3 is used to clamp the reverse recovery spike across the auxiliary switch when the inductor current returns to zero (t_4 in Fig. 11). The circuit operates the same as method D to turn the main switch on with zero voltage. However, when the main switch is turned-off the output current will not only charge C_1 but it will discharge C_r through the diode D_2 . When the voltage across C_r has reached zero volts the diode D will then conduct. Therefore, the energy stored in C_1 before the main switch was turned on is transferred to C_r and eventually is transferred to the output when the main switch is turned off. Furthermore, because the C_r capacitor voltage is zero at the start of each cycle, the peak currents thought the auxiliary circuit are lower giving smaller conduction losses than method D. With these added diodes, the auxiliary switch, S_r , has turn-on losses identical to methods B and C and turn off losses identical to methods A and D. Furthermore, the danger of the auxiliary switch voltage breakdown has been eliminated.

IV. EXPERIMENTAL SETUP AND PROCEDURE

A 250kHz switching frequency experimental circuit with the above described soft-switching methods was built to compare their performance characteristics. Each experiment used the same base boost circuitry while the auxiliary circuit modules were applied. This ensured identical layout topologies for the power switches. Furthermore, each test used the same thermal management setup. Additionally, under the constraint that the auxiliary circuit conduction time was less than 25% of the switching period, the circuit components (L_r and C_r) of each method were adjusted to obtain the highest experimental efficiencies at 600 Watts of output power and input and output voltages at 100 and 300 volts respectively. All circuit diodes were MUR860s; the input inductor of the boost converter, L , was 200μH; and the output capacitor, C_o , was 200μF; the main switch was an IRFP450 and the auxiliary switch was an IRFP840. The other

circuit parameters are shown in the schematics (Figs. 6,8,9,10,12).

The efficiency of each method was measured from 100-700 Watts range of output power with approximate input voltage at 100 volts and output voltage at 300 volts using a Tektronix 2505 Data Acquisition TestLab. Using four 12 bit A/D channels sampling at 100kHz, the DC input voltage and current and output voltage and current were simultaneously measured. The range and offset of the differential amplifiers within the TestLab were adjusted to achieve the highest A/D resolution possible. Although the DC input supply was regulated, line frequency ripple was still detectable. Therefore, to eliminate the influence of the ripples in the efficiency measurements, each test consisted of five 60Hz line cycles (8333 samples) where instantaneously input and output power were calculated and then averaged. This experimental setup ensured a very repeatable and stable system to perform the measurements.

To accurately compare each soft-switching method at the appropriate power level, the input current and output voltage were adjusted to be identical for each converter. As discussed in section II, the losses associated with the auxiliary circuit are dependent on the input current I_s and output voltage $V_b=V_o$. By equalizing these test parameters, an accurate comparison between the converters can be achieved. The duty ratio and input voltage were adjusted slightly for each method to achieve this test condition.

V. EXPERIMENTAL RESULTS AND OBSERVATIONS

Figures 13, 14, 15, 16, 17 show that each method turns on the main switch (see V_{ds1} & V_{gs1}) with zero voltage and that the drain voltage rising edge is slowed by the snubber capacitor C_1 . The time that the auxiliary switch is turned on also can be indirectly taken from the figures by correlating it with the time the auxiliary inductor current begins to rise. Although methods A, B, and C included a saturable inductor, this blocking time is very short and can be neglected. Fig. 18. shows the waveforms for the hard switched converter. In contrast to the soft switched methods, the hard switched converter is not turned on with zero voltage and the device has a very large power dissipation spike at each switching interval.

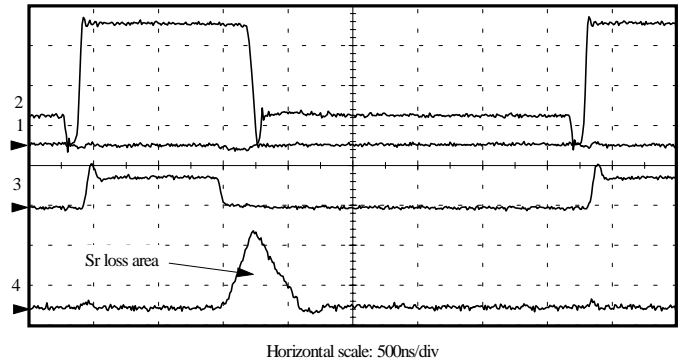


Fig. 13. Soft-switching method A: 600 Watts output power. 1: V_{ds1} 100v/div; 2: V_{gs1} 20v/div; 3: V_{dsr} 275v/div; 4: I_{Lr} , 5A/div

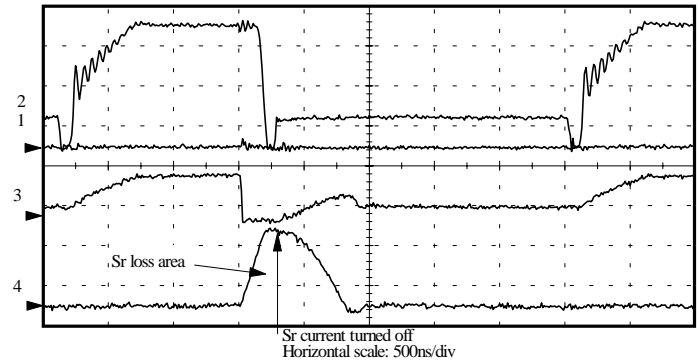


Fig. 14. Soft-switching method B: 600 Watts output power. 1: V_{ds1} 100v/div; 2: V_{gs1} 20v/div; 3: V_{dsr} 275v/div; 4: I_{Lr} 5A/div

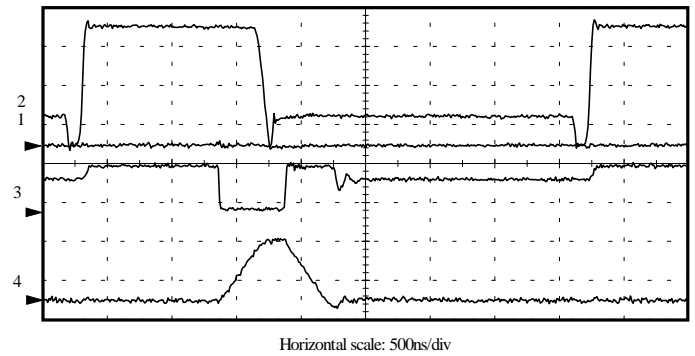


Fig. 15. Soft-switching method C: 600 Watts output power. 1: V_{ds1} 100v/div; 2: V_{gs1} 20v/div; 3: V_{dsr} 275v/div; 4: I_{Lr} 5A/div

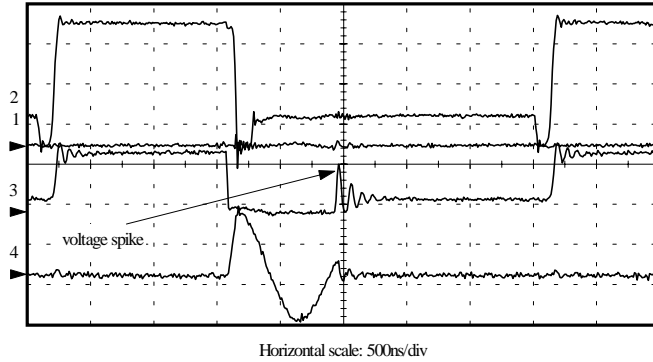


Fig. 16. Soft-switching method D: 600 Watts output power. 1: V_{ds1} 100v/div; 2: V_{gs1} 20v/div; 3: V_{dsr} 275v/div; 4: I_{Lr} 10A/div

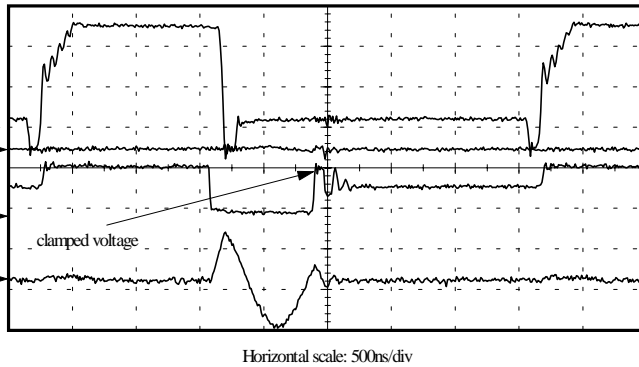


Fig. 17. Soft-switching method E: 600 Watts output power. 1: V_{ds1} 100v/div; 2: V_{gs1} 20v/div; 3: V_{dsr} 275v/div; 4: I_{Lr} 10A/div

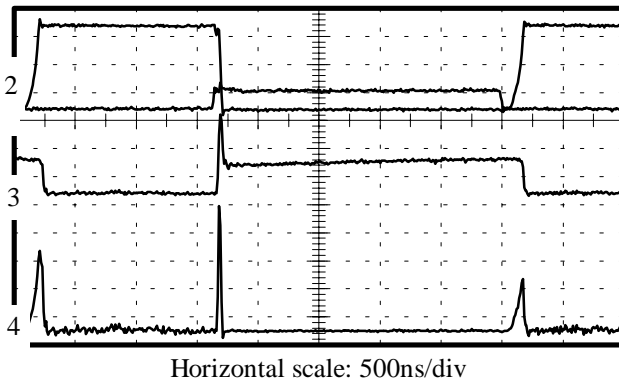


Fig. 18. Hard switched converter: 600 Watts output power. 1: V_{ds1} 100v/div; 2: V_{gs1} 20v/div; 3: I_{S1} : 5 A/div; 4: P_{S1} : 4.25kW/div

Table 1 gives a first order loss comparison between the different methods. In this comparison, the four major losses associated with the auxiliary circuit were included and

assumed to have equal weight and independent of one another. For each loss, the methods were ranked from highest to lowest efficiency. For example, the turn-on loss of method A is the smallest of all converters, followed by methods B, C and E for second, and finally method D for last. The total in Table 1 for this first order comparison shows that methods A and B are the highest in efficiency, followed by methods C and E, and then method D. The actual efficiency results show this basic performance grouping.

The efficiency of each soft-switching method and the hard switched converter are shown in Fig. 19. These results are slightly different from those presented in [1]. This difference is because for the given results, the circuit parameters were experimentally optimized for 600Watts output power and the circuit cooling was standardized as mentioned in Section IV of this paper. For the hard switched converter, the snubber capacitor, C_1 , across the main switch S_1 was removed. Figure 19. shows that methods A and B are the most efficient soft-switching techniques. Method A obtained the highest efficiency at low power and method B performed the best at high power. As explained before, method A has the lowest auxiliary switch turn-on loss of any converter. This factor makes it the best technique at lower power. However, when power increases, the conduction loss due to the 1Ω auxiliary switch resistance becomes significant, thus method B dominates. For method B, the auxiliary switch is only on for the first part of the cycle. Looking at the waveforms Figs. 13 and 14, one can see that the area under the inductor current (S_r switch current) of method A is larger than the area under the switch conduction time of method B. Furthermore, method A transfers the energy from its auxiliary circuit to the input instead of the output like method B; therefore, this part of the energy is processed twice before it reaches the output. This becomes significant when it is operating at high current. These factors cause the efficiency decrease of method A at high power. At low power (200-300 Watts), the hard switched converter has the highest efficiency of all the methods except A and B. For the other converters, although soft-switching of the main switch is maintained at lower power, the energy savings is less than the losses caused by the auxiliary circuits themselves! At higher power, method E has the third highest efficiency and shows the 3-4% improvement it makes over method D by transferring the capacitor energy to the output each cycle. Method D's performance is severely hampered by the dissipated energy within the auxiliary circuit and does not improve efficiency over the hard switched converter until very high power. Although the waveforms of method C are very close to method B (see Figs. 14 and 15.), the fact that the auxiliary switch in method C is turned off dissipatively accounts its lower performance.

METHOD	A	B	C	D	E
INDUCTOR ENERGY TRANSFER LOSS	2	1	1	3	1
TURN ON LOSS	1	2	2	3	2
TURN OFF LOSS	1	2	3	1	1
CONDUCTION LOSS	2	1	1	3	3
TOTAL	6	6	7	10	7

Table 1. First order loss comparison

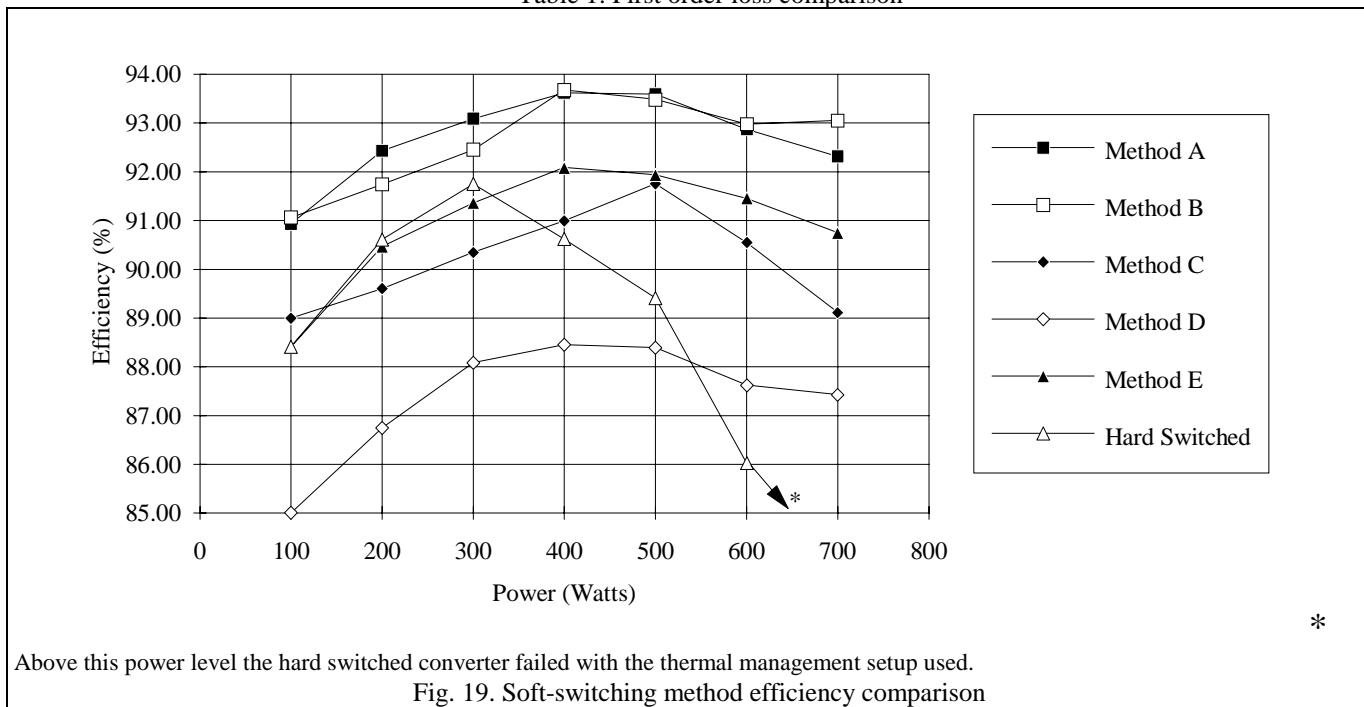


Fig. 19. Soft-switching method efficiency comparison

Figure 16. shows a substantial voltage spike across the auxiliary switch (V_{dsr}) for method D. This is caused by the reverse recovery time of the anti-parallel diode. Figure 17 shows how method E uses diode D_3 to clamp this reverse recovery spike to the output voltage. Furthermore, it is evident from this figure why the efficiency of method E is lower than methods A and B. The LC resonance peak current is higher causing more conduction loss in the auxiliary circuit. Also, the negative current in the resonant inductor add to the main switches conduction loss more than tripling the input current during this period. Even though the conduction time of this current hump is small, compared to methods A and B, it is not the optimum configuration for efficiency. On the

other hand, because method E's auxiliary switch is softly turned off, the excess conduction losses are still better than the dissipative switch turn-off loss of method C.

VI. CONCLUSIONS

Five voltage-mode soft-switching methods were compared and experimentally analyzed. Methods A and E emerged during this study by the authors with method A being similar to prior work in [6]. Methods A and B showed the highest efficiency. Method A did well at low power levels, and method B did well at higher power levels. Although method A has a limited zero voltage range ($V_o/V_{in} > 2$) and requires a isolated gate drive, the number of

components is the least of any of the converters. Method B has the most components, but always provides zero voltage switching and high efficiency over the complete power range. Method E showed excellent improvement over method D, but still does not meet the efficiencies of methods A and B. Method C exhibits lower efficiency than method B due to its dissipative turn off of the auxiliary switch. Methods D has the lowest efficiency and extra care must be taken to make sure the efficiency has improved over the hard switching converter. The best methods improve efficiency over the hard switched converter by softly switching the auxiliary switch, minimizing the amount of redirection current, and recovering the auxiliary circuit energy.

An observation worth mentioning was the radiated EMI improvement method A appeared to have over the other converters. During all experiments an FM radio was placed within ten feet of the converter. At 600 Watts of output power the only converter that did not experience any radio interference was method A.

High frequency power conversion has some obvious advantages, but at a price. The increased switching frequency

causes the switching losses to become very substantial. Therefore, solutions must be found to reduce this loss. Voltage-mode soft-switching converters have been shown to provide very good efficiency improvements of the main switch turn-on and turn-off periods. And most of them will improve overall circuit efficiency within a certain power range. But until now, understanding a soft-switching circuit's advantages and disadvantages over another techniques has been vague at best. By comparing the selected promising methods, an understanding of the loss mechanisms and selected circuit advantages has been improved.

ACKNOWLEDGMENT

The authors would like to thank Zheren Lai and the other members of the Power Electronics Lab at UCI for many valuable suggestions and discussions. Equipment support by the Tektronix Seed Grant was indispensable for this research. Furthermore, component support from Harris Semiconductor and Motorola was greatly appreciated. Special thanks goes to the reviewers whose suggestions were invaluable for the revision of this paper.

REFERENCES

- [1] K. M. Smith and K. M. Smedley, "A comparison of voltage mode soft switching methods for PWM converters," IEEE APEC Conf. Rec., 1996, pp. 291-8 vol. 1.
- [2] R. Streit and D. Tollik "High efficiency telecom rectifier using a novel soft-switched boost-based input current shaper," IEEE Intelec Conf. Rec., 1991, pp.720-726.
- [3] S. Ben-Yaakov, G. Ivensky, O. Levitin and A. Treiner, "Optimization of the auxiliary switch components in a flying capacitor ZVS PWM converters," IEEE APEC Conf. Rec., 1995, pp. 503-509.
- [4] G. Hua, C. Leu, Y. Jiang, and F. Lee, "Novel zero-voltage-transition PWM converters," IEEE Trans. on Power Electronics, Vol. 9, No. 2, March 1994.
- [5] G. Moschopoulos, P. Jain, and G. Joos, "A novel zero-voltage switched PWM boost converter," IEEE PESC Conf. Rec., 1995, pp. 695-700.
- [6] L. Freitas, and P. Gomes, "A High-Power High-Frequency ZCS-ZVS-PWM Buck Converter Using A Feedback Resonant Circuit," IEEE PESC Conf. Rec., 1993, pp. 330-336.
- [7] Gegner, J. , and C. Lee, "Zero-voltage-transition converters using an inductor feedback technique," IEEE APEC Conf. Rec., 1994, pp. 862-868.
- [8] K. Harada, H. Sakamoto, and K. Harada, "Saturable inductor commutation for zero voltage switching in DC-DC converter," IEEE Trans. on Magnetics, Vol. 26, No. 5, Sep. 1990.
- [9] M. Brkovic, A. Peitkiewicz, and S. Cuk, "Novel Soft-Switching Converter with Magnetic Amplifiers," IEEE Intelec Conf. Rec., 1994, pp. 155-162.
- [10] M. Brkovic, A. Peitkiewicz, and S. Cuk, "Novel Soft-Switching Full-Bridge Converter With Magnetic Amplifiers", IECON Conf. Rec., 1993, pp. 830-835.
- [11] G. Hua, F. Lee, and M. Jovanovic, "An improved zero-voltage-switched PWM converter using a saturable inductor", IEEE PESC Rec, 1991, pp. 189-194.
- [12] R. Farrington, M. Jovanovic, and F. Lee, "A new family of isolated zero-voltage-switched converters," IEEE PESC Conf. Rec. , 1991, pp. 209-215.
- [13] K. Wang, F.C. Lee, G. Hua, and D. Borojovic, "A comparative study of switching losses of IGBTs under hard-switching, zero-voltage-switching and zero-current-switching," IEEE PESC Conf. Rec., 1994, pp. 1196-1204.
- [14] C. Canesin, and I. Barbi, "Comparison of experimental losses among six different topologies for a 1.6kW boost converter, using IGBT's," IEEE PESC Conf. Rec., 1995, pp. 1265-1271.
- [15] J. Kassakian, M. Schlecht, G. Verghese, *Principles of Power Electronics*. Addison-Wesley Publishing Company, Reading Massachusetts, 1991.